Application of Hypoxia to Establish Epithelial-Mesenchymal Transition Models in Renal Cell Carcinoma Cell Lines

Baoan Hong[2], Changhua Zhou[3], Xin Du[4], Siqi Chen[3], Xiaohu Deng[5], Shayiremu Duoerkun[6], Qing Li[3], Yong Yang[1], Kan Gong[2] and Ning Zhang[1]*

[1]Department of Urology, Peking University Cancer Hospital, Beijing Institute for Cancer Research, Beijing, P.R. China
[2]Department of Urology, Peking University First Hospital, Beijing, P.R. China
[3]School of Pharmaceutical Sciences, Center for Cellular and Structural Biology, Sun Yat-Sen University, Guangzhou, P.R. China
[4]Department of Urology, Beijing Chaoyang Hospital, Capital Medical University, Beijing, P.R. China
[5]Department of Urology, Karamay People's Hospital, Xinjiang, P.R. China
[6]Department of Urology, Hami District Central Hospital, Xinjiang, P.R. China

Abstract

Purpose: To establish epithelial-mesenchymal transition (EMT) models in renal cell carcinoma cell lines by $CoCl_2$-induced hypoxia.

Materials and methods: The renal cell carcinoma cell lines A498 and 786-O were used in the experiment and $CoCl_2$ was used to simulate hypoxia. The cancer cells were cultured with different concentrations of $CoCl_2$. Morphology and cyto-activity changes were detected to obtain the optimal concentration of $CoCl_2$ for simulating hypoxia. After $CoCl_2$ treatment, the cells were subjected to Western blot analysis to test the expression of HIF-1α and the changes of EMT-related molecules (E-cadherin, fibronectin).

Results: Cell conjunctions of $CoCl_2$-treated groups were loose and scattered compared to the control. The effect of $CoCl_2$ on A498 cell viability was not distinct at a low dosage, but when the concentration of $CoCl_2$ reached 250 mM, cell activity gradually declined. In contrast, $CoCl_2$ induced 786-O cell proliferation in the range of 50 mM-200 mM, but it inhibited cell growth at dosages higher than 200 mM. The expression of E-cadherin was significantly down-regulated, and fibronectin was up-regulated in both A498 and 786-O cell lines under $CoCl_2$-simulated hypoxia in comparison with normoxic conditions (P<0.01).

Conclusions: EMT models of the renal cell carcinoma cell lines were successfully established by $CoCl_2$-induced hypoxia. The models will help us further study the mechanisms of EMT and investigate novel therapeutic targets to inhibit tumor invasion and metastasis.

Introduction

Kidney cancer originating from the renal tubular epithelium system is one of the most common cancers of the urinary system. It accounts for approximately 3% of all malignant tumors. The incidence of newly diagnosed patients has increased by approximately 2.5-3% annually from 2001-2010 [1,2]. Metastatic renal cell carcinoma is detected in approximately 30% of patients at the time of diagnosis [3]. The overall distribution of metastatic sites is the lung, bone, lymph nodes, liver, adrenal gland and brain [4]. Metastatic renal cell carcinoma has a poor prognosis with a median overall survival of 12 months and a 5-year survival rate of less than 10%, which seriously affects patients' quality of life [5]. Invasion and metastasis, the major characteristics of malignant tumors, lead to the poor prognosis and death of patients. At present, the intrinsic molecular mechanisms and the extrinsic microenvironment that enhance the metastatic potential of primary tumor cells are still hot topics in the field of cancer research. Remarkably, a multitude of studies have revealed that activation of epithelial-mesenchymal transition (EMT) endows metastatic properties upon cancer cells to promote invasion, migration, and subsequent dissemination [6-12]. EMT is a process known as epithelial phenotype transdifferentiation into mesenchymal phenotype. During the EMT, cellular morphology and adhering capacity will change and the expression of epithelial molecular markers will down-regulate while that of mesenchymal molecular markers will increase. Hypoxia, one of the various factors that can induce EMT in cancer cells, exists in many regions of solid tumors [13,14] because angiogenesis in tumors

is heterogeneous, and cancer cells grow rapidly. If an EMT model can be successfully established with a hypoxic microenvironment *in vitro*, it will provide support to study the mechanisms of tumor invasion and metastasis. Currently, there is no relevant EMT model in the field of renal cell carcinoma. In this study, the renal cell carcinoma cell lines A498 and 786-O were incubated with cobaltous chloride ($CoCl_2$). We monitored the process of the EMT from three aspects: characteristics of cell growth, the expression of hypoxia-inducible factor-1α (HIF-1α) and the expression changes of EMT-related molecules.

Materials and Methods

Cell lines and cell culture

Renal cell carcinoma A498 and 786-O cells were provided by Sun Yat-Sen University Laboratory (Guangzhou, China). Both are adherent epithelial human renal cell carcinoma cell lines with a generation time of 2-3 days. They were cultured in a humidified incubator

(Thermo Scientific, USA) at 37°C, 5% CO_2. A498 cells were cultured in Dulbecco's modified Eagle's medium (DMEM) (Hyclone, USA) supplemented with 10% fetal bovine serum (Hyclone, USA), 100 U/mL penicillin and 100 μg/mL streptomycin (Gibco, USA); 786-O cells were cultured in RPMI-1640 medium (Hyclone, USA) supplemented with 10% fetal bovine serum (Hyclone, USA), 100 U/mL penicillin and 100 μg/mL streptomycin (Gibco, USA). For experiments requiring hypoxia, $CoCl_2$ (Sangon, Shanghai) was added to simulate a hypoxic microenvironment.

Effects of CoCl$_2$ on cell growth

Cancer cells were harvested during the logarithmic growth period and counted by Countstar (Inno-Alliance Biotech, USA). The cell concentration was adjusted to 5.0×10^4/mL with the respective culture medium. Cell suspensions, approximately 100 μL/well, were seeded in 96-well plates (Corning Costar, USA) and cultured in a humidified incubator at 37°C, 5% CO_2 for 24 h. Then, 10 μl of $CoCl_2$ at different concentrations was added to each well, making final concentrations of 0 μM, 50 μM, 100 μM, 150 μM, 200 μM, 250 μM, 300 μM, 400 μM, 800 μM. During the process of culturing, cellular morphology was observed under an inverted microscope (Olympus CKX41SF, Japan), and cyto-activity was tested by Cell Counting Kit-8 (Dojindo, Japan) at 24 h, 48 h, 72 h, 96 h and 120 h.

Effects of CoCl$_2$ on the expression of HIF-1α

Cancer cells were harvested during the logarithmic growth period, counted by Count star and adjusted to 1.0×10^5/mL with the respective culture medium. Cell suspensions, approximately 2 mL/well, were seeded in 6-well plates (Corning Costar, USA) and cultured in a humidified incubator at 37°C, 5% CO_2 for 24 h. Then, to every well 200 μL of different concentrations of $CoCl_2$ was added, making final concentrations of 50 μM, 100 μM, 200 μM, 400 μM, 800 μM. Each sample had set a blank control group. After treatment with $CoCl_2$, the plates were incubated for 72 h and then the total protein was extracted for Western Blot assays to test the expression of HIF-1α in tumor cells.

The cells were lysed in lysis buffer for approximately 15 min, and the lysed cells were centrifuged for 15 min at 12,000 rpm. Protein quantification was determined using the bicinchoninic acid (BCA) colorimetric assay (Pierce BCA Protein Assay Kit, Thermo Scientific, USA). Proteins (10 μg) undergoing sodium dodecyl sulfate polyacrylamide gel electrophoresis (SDS-PAGE) were transferred to a PVDF membrane (Invitrogen, USA) by electroblotting. The membranes were incubated in TBST (10 mM TBS and 0.05% Tween 20) supplemented with 5% fat-free milk at room temperature for 1 h. Next, the membranes were placed in a bull serum albumin diluted solution containing the primary antibody HIF-1α (1:1000, #14179, cell signaling, USA) or α-Tubulin (1:1000, #2125, cell signaling, USA) and reacted at 4°C overnight. After repeated washing, the membranes were incubated with secondary Anti-Rabbit IgG, HRP-linked Antibody (1:2000, #7074, cell signaling, USA) and enhanced electrochemiluminescence (ECL) detection reagent. The above experiment was repeated at least 3 times. The bands were detected using the enhanced chemiluminescence system (Bio-Rad, USA).

Effects of CoCl$_2$ on EMT-related molecular changes

Cancer cells were harvested during the logarithmic growth period, counted by Count star and adjusted to 1.0×10^5/mL with the respective culture medium. Cell suspensions, approximately 2 mL/well, were seeded in 6-well plates and cultured in a humidified incubator at 37°C, 5% CO_2 for 24 h. Referring to the results of observing cell morphology,

activity and expression of HIF-α in the experiment above, 200 μL of $CoCl_2$ was added to every well to make a final concentration of 200 μM. The plates were incubated for 72 h, and the total protein was extracted for Western Blot assays to test the changes of EMT-related molecules.

The Western blotting procedure was the same as above. However, the primary antibodies were fibronectin (1:1000, ab6328, abcam, UK), E-cadherin (1:1000, 5296s, cell signaling, USA), and α-tubulin (1:1000, #2125, cell signaling, USA), and the secondary antibody was Anti-Rabbit IgG, HRP-linked Antibody (1:2000, #7074, cell signaling, USA). The above experiment was repeated at least 3 times. In each group, α-tubulin was regarded as the loading control. Image J software was used to calculate the luminance values of target Western blot protein bands and compare them with an internal reference to obtain the luminance ratio.

Statistical analysis

All of the statistical analysis was performed with SPSS 19.0 software. The measurement data were reported as the mean ± standard deviation $(x \pm s)$. Comparisons among data sets were made with Student's t-test. Differences were considered to be statistically significant when the P value was <0.05.

Results

Characteristics of cell growth

A498 and 786-O cells were cultured in normal medium or supplemented with $CoCl_2$. After 72 h, cell conjunctions between 786-O cells were much looser and more scattered in the groups with added $CoCl_2$ than in the blank control group (Figure 1A and 1B). However, A498 cells showed the same characteristics in cell growth after 96 h (Figure 1C and 1D).

Effects of CoCl$_2$ on cell viability

The effects of $CoCl_2$ on the viability of A498 cells were not distinct at low dosage, but when the concentration increased to 250 μM, cell activity gradually declined. For example, when the concentration was 250 μM, relative cell viability decreased from 85%-50% from 24 h - 120 h (Figure 2). However, when the concentration of $CoCl_2$ ranged from 50 μM-200 μM, it obviously stimulated 786-O cells to proliferate. When the concentration exceeded 250 μM, it produced inhibitory effects on cell viability. For example, relative cell viability remained below 100% from 24 h - 120 h at the concentration of 250 μM (Figure 3).
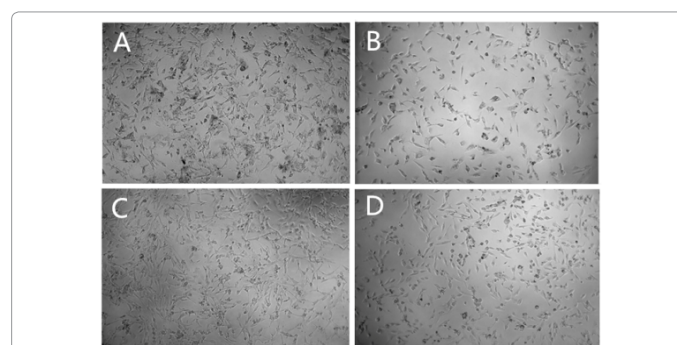

Figure 1: Morphological changes during the process of cell culture (X200). A. Morphological changes in the blank control group of 786-O cells (72 h), B. Morphological changes in the CoCl2-treated group of 786-O cells (72 h), C. Morphological changes in the blank control group of A498 cells (96 h), D. Morphological changes in the CoCl2-treated group of A498 cells (96 h).

Expression of HIF-1α

When cultured with different concentrations of $CoCl_2$ for 72 h, the expression quantity of HIF-1α in A498 cells was significantly increased with increasing $CoCl_2$ concentration, and the difference was significant compared with the blank control group (Figure 4). Expression of HIF-1α was not observed in 786-O cells whether cultured in normoxic conditions or treated with $CoCl_2$ for 72 h.

Changes of EMT-related molecules

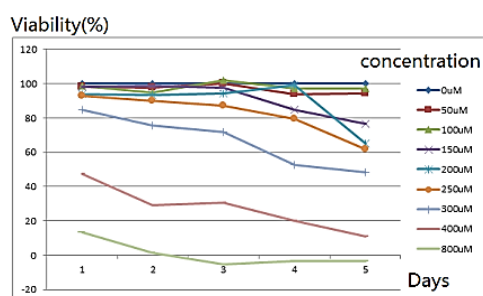In the process of culture, we had observed that when the

Figure 2: Effects of different concentrations of CoCl2 on A498 cell activity. The cell activity of the blank control group was set as the baseline.
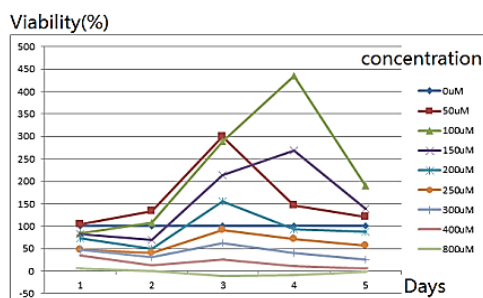

Figure 3: Effects of different concentrations of $CoCl_2$ on 786-O cell activity. The cell activity of the blank control group was set as the baseline.
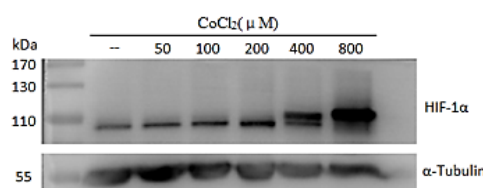

Figure 4: Effects of different concentrations of $CoCl_2$ on the expression of HIF-1α in A498 cells.
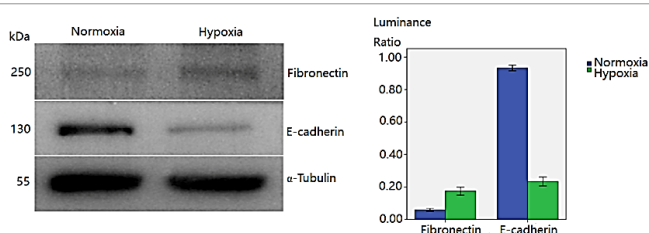

Figure 5: Normoxia (blank control group) or hypoxia ($CoCl_2$-treated group) culture for 72 h, E-cadherin and fibronectin expression in the A498 cell line.
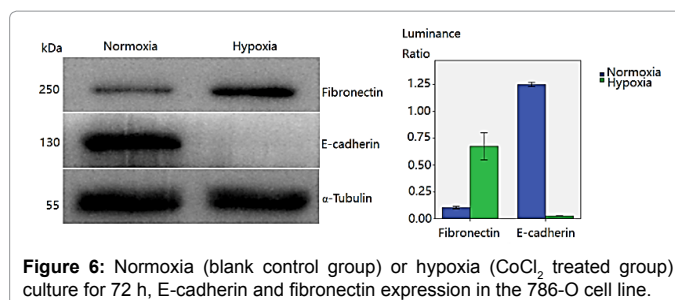

Figure 6: Normoxia (blank control group) or hypoxia ($CoCl_2$ treated group) culture for 72 h, E-cadherin and fibronectin expression in the 786-O cell line.

concentration of $CoCl_2$ was 200 μM and cells were cultured for 72 h, the two cell lines grew well, and their intercellular structure changed significantly, such as cell conjunctions being looser and scattered. Therefore, we selected the culture conditions above to simulate a hypoxic microenvironment. The results indicated that for the blank control group and $CoCl_2$-treated group in the A498 cell line, the luminance ratio of E-cadherin expression was 0.934 ± 0.402 and 0.234 ± 0.616, respectively, and the luminance ratio of fibronectin expression was 0.059 ± 0.168 and 0.175 ± 0.049, respectively. The differences between the two groups were considered to be statistically significant (P<0.01) (Figure 5). For the blank control group and the $CoCl_2$-treated group in the 786-O cell line, the luminance ratio of E-cadherin expression was 1.250 ± 0.435 and 0.026 ± 0.004, respectively, and the luminance ratio of fibronectin expression was 0.104 ± 0.022 and 0.674 ± 0.253, respectively. The differences between the two groups were considered to be statistically significant (P<0.01) (Figure 6).

Discussion

The EMT is a wide range of biological processes that al-low a polarized epithelial cell to undergo multiple biochemi-cal changes that enable it to assume a mesenchymal cell pheno-type, which includes enhanced migratory capacity, invasiveness and resistance to apoptosis. In 1982, Greenburg and Hay [15] re-vealed that environmental conditions have profound effects on the epithelial phenotype, the cell shape and the polarity as expressed by the presence of apical and basal surfaces. The EMT exists in many basic physiological and pathological processes, divided into three subtypes: 1) association with implantation, embryo formation, and organ de-velopment; 2) association with tissue regeneration and organ fibrosis; and 3) existence in cancer progression and metastasis [16]. In recent years, the EMT was found in gastrointestinal cancer, pancreatic can-cer, liver cancer, prostate cancer, breast cancer and other tumors and is associated with tumor infiltration and metastasis [17-23]. Zhang et al. [14] demonstrated that hypoxia was able to induce the EMT and enhance the ability of invasion and migration in HCC cells. Huang et al. [24] also reported that upregulation of HIF-1α, together with EMT alteration, resulted in increased migration and invasion of HepG2 cells under hypoxia. Chu et al. [25] showed that the underlying mechanism of tumor progression in breast cancer might be associated with the ep-ithelial-mesenchymal transition (EMT). Therefore, further study of the EMT will help us understand the molecular mechanism of tumor me-tastasis and provide a potential therapeutic target for cancer treatment.

Hypoxia is an important factor inducing EMT in tumors. Solid tumors grow in hypoxic conditions, which exert critical effects on the gene phenotype of tumor cells. Tumor growth and metastasis are promoted by a variety of pathways involved in affecting metabolism, activating tumor growth factors, promoting drug or radiation resistance, and enhancing malignant biological behavior [26-28]. An important mechanism by which hypoxia promotes the invasion and metastasis of

malignant tumors is according to the regulation of the EMT process. Under hypoxic conditions, a series of changes of cytokines occur in tumor cells. Studies have demonstrated that HIFs are key transcription factors that transmit hypoxic signals and mediate hypoxia effects [29-31]. They mediate many links within tumor invasion and metastasis by combining with hypoxia response elements and activating downstream target genes. Meanwhile, HIFs also play an important role in inducing the EMT in a variety of ways [32-36].

In this study, we applied $CoCl_2$ to simulate hypoxia. Co^{2+} is a substrate of the iron chelating enzyme; it can replace the Fe^{2+} in the oxygen sensor of heme and prevent the oxygen sensor from combining with oxygen. Then, the tumor cells would "feel" a lack of oxygen in normoxia and consequently up-regulate the expression of hypoxia inducing factors [25,37-39]. During the process of culturing, the effect of $CoCl_2$ on the viability of A498 cells was not distinct at lower dosage. When the concentration of $CoCl_2$ reached 250 μM, cell activity significantly declined. This finding suggested that A498 cells were more tolerant of $CoCl_2$-induced hypoxia. In contrast, 50 μM-200 μM of $CoCl_2$ stimulated the proliferation of 786-O cells. However, dosages higher than 200 μM had an inhibitory effect on cell growth. Therefore, the different cell lines showed diverse tolerance profiles to $CoCl_2$-induced hypoxia.

To identify the occurrence of the EMT, we monitored the changes of cell morphology and detected the expression of HIF-1α and EMT-related molecular markers. $CoCl_2$-treated tumor cells appeared looser and scattered from cell-to-cell junctions. These changes allowed the epithelial cells to break away from intercellular junctions and become migratory and aggressive. In addition, HIF-1α expression in A498 cells significantly increased in a $CoCl_2$-dose-dependent manner. However, HIF-1α expression was not observed in 786-O cells. It was reported that certain VHL-defective cells, 786-O, did not express detectable HIF-1α [40]. This again demonstrates that renal carcinoma cell lines with different biological characteristics have different responses to hypoxia. Hypoxic conditions could induce the EMT through different signaling pathways [35,36].

The epithelial phenotype turning into a mesenchymal phenotype is an important characteristic of the EMT. Another critical signature of the EMT is the reduction or loss of E-cadherin [41]. E-cadherin is an intercellular adhesion molecule that belongs to the type-I adhesive proteins and calcium-dependent trans membrane glycoproteins in epithelial tissues. It can promote connections between cells, maintaining the cytoskeleton and the stability of attachment brackets. A number of transcription factors directly or indirectly inhibit the expression of E-cadherin or prevent it from interacting with itself, which results in EMT [11,42-44]. Loss or reduction of E-cadherin has a significant influence on cellular functions, including loss of cell polarity and decreased cell adhesion ability. In recent years, many studies have shown that the aberrant activation of EMT promotes tumor metastasis by repressing cell adhesion molecules, such as E-cadherin [45,46]. Reduced intracellular adhesion allows tumor cells to disseminate and spread throughout the body. When the EMT process starts, the expression of mesenchymal phenotype related molecules will be up-regulated. We found that the expression of E-cadherin was significantly down-regulated, and fibronectin was up-regulated in both A498 and 786-O cell lines under $CoCl_2$-induced hypoxia.

In conclusion, we have successfully generated EMT models by incubation of the renal carcinoma cell lines A498 and 786-O with $CoCl_2$. The models will help us and other researchers not only further study the mechanisms of the EMT but also investigate novel therapeutic targets to inhibit tumor invasion and metastasis.

References

1. King SC, Pollack LA, Li J, King JB, Master VA (2014) Continued increase in incidence of renal cell carcinoma, especially in young patients and high grade disease: United States 2001 to 2010. J Urol 191: 1665-1670.

2. Ohba K, Miyata Y, Mitsunari K, Matsuo T, Mochizuki Y, et al. (2014) Left atrial metastasis of renal cell carcinoma: a case report and review of the literature. BMC Res Notes 7: 520.

3. Fisher R, Gore M, Larkin J (2013) Current and future systemic treatments for renal cell carcinoma. Semin Cancer Biol 23: 38-45.

4. Bianchi M, Sun M, Jeldres C, Shariat SF, Trinh QD, et al. (2012) Distribution of metastatic sites in renal cell carcinoma: a population-based analysis. Ann Oncol 23: 973-980.

5. Liu L, Zhang W, Qi X, Li H, Yu J, et al. (2012) Randomized study of autologous cytokine-induced killer cell immunotherapy in metastatic renal carcinoma. Clin Cancer Res 18: 1751-1759.

6. De Craene B, Berx G (2013) Regulatory networks defining EMT during cancer initiation and progression. Nat Rev Cancer 13: 97-110.

7. Gao D, Joshi N, Choi H, Ryu S, Hahn M, et al. (2012) Myeloid progenitor cells in the premetastatic lung promote metastases by inducing mesenchymal to epithelial transition. Cancer Res 72: 1384-1394.

8. Lamouille S, Xu J, Derynck R (2014) Molecular mechanisms of epithelial-mesenchymal transition. Nat Rev Mol Cell Biol 15: 178-196.

9. Polyak K, Weinberg RA (2009) Transitions between epithelial and mesenchymal states: acquisition of malignant and stem cell traits. Nat Rev Cancer 9: 265-273.

10. Scheel C, Eaton EN, Li SH, Chaffer CL, Reinhardt F, et al. (2011) Paracrine and autocrine signals induce and maintain mesenchymal and stem cell states in the breast. Cell 145: 926-940.

11. Thiery JP, Acloque H, Huang RY, Nieto MA (2009) Epithelial-mesenchymal transitions in development and disease. Cell 139: 871-890.

12. Wong IY, Javaid S, Wong EA, Perk S, Haber DA, et al. (2014) Collective and individual migration following the epithelial-mesenchymal transition. Nat Mater 13: 1063-1071.

13. Matsuoka J, Yashiro M, Doi Y, Fuyuhiro Y, Kato Y, et al. (2013) Hypoxia stimulates the EMT of gastric cancer cells through autocrine TGFβ signaling. PLoS One 8: e62310.

14. Zhang L, Huang G, Li X, Zhang Y, Jiang Y, et al. (2013) Hypoxia induces epithelial-mesenchymal transition via activation of SNAI1 by hypoxia-inducible factor-1 alpha in hepatocellular carcinoma. BMC Cancer 13: 108.

15. Greenburg G, Hay ED (1982) Epithelia suspended in collagen gels can lose polarity and express characteristics of migrating mesenchymal cells. J Cell Biol 95: 333-339.

16. Kalluri R, Weinberg RA (2009) The basics of epithelial-mesenchymal transition. J Clin Invest 119: 1420-1428.

17. Byles V, Zhu L, Lovaas JD, Chmilewski LK, Wang J, et al. (2012) SIRT1 induces EMT by cooperating with EMT transcription factors and enhances prostate cancer cell migration and metastasis. Oncogene 31: 4619-4629.

18. Chen J, Imanaka N, Chen J, Griffin JD (2010) Hypoxia potentiates Notch signaling in breast cancer leading to decreased E-cadherin expression and increased cell migration and invasion. Br J Cancer 102: 351-360.

19. Jiao L, Li DD, Yang CL, Peng RQ, Guo YQ, et al. (2016) Reactive oxygen species mediate oxaliplatin-induced epithelial-mesenchymal transition and invasive potential in colon cancer. Tumour Biol 37: 8413-8423

20. Joo YE, Park CS, Kim HS, Choi SK, Rew JS, et al. (2000) Prognostic significance of E-cadherin/catenin complex expression in gastric cancer. J Korean Med Sci 15: 655-666.

21. Krantz SB, Shields MA, Dangi-Garimella S, Munshi HG, Bentrem DJ (2012) Contribution of epithelial-to-mesenchymal transition and cancer stem cells to pancreatic cancer progression. J Surg Res 173: 105-112.

22. Tai CJ, Chin-Sheng H, Kuo LJ, Wei PL, Lu HH, et al. (2012) Survivin-mediated cancer cell migration through GRP78 and epithelial-mesenchymal transition (EMT) marker expression in Mahlavu cells. Ann Surg Oncol 19: 336-343.

23. Zuo J, Wen J, Lei M, Wen M, Li S, et al. (2016) Hypoxia promotes the invasion and metastasis of laryngeal cancer cells via EMT. Med Oncol 33: 15.

24. Huang MS, Wang L, Chen JW, Bai MJ, Zhou CR, et al. (2016) Regulation of COX-2 expression and epithelial-to-mesenchymal transition by hypoxia-inducible factor-1a is associated with poor prognosis in hepatocellular carcinoma patients post TACE surgery. Int J Oncol. 48: 2144-2154.

25. Chu CY, Jin YT, Zhang W, Yu J, Yang HP, et al. (2016) CA IX is upregulated in CoCl2-induced hypoxia and associated with cell invasive potential and a poor prognosis of breast cancer. Int J Oncol 48: 271-280.

26. Carmeliet P (2003) Angiogenesis in health and disease. Nat Med 9: 653-660.

27. Harris AL (2002) Hypoxia--a key regulatory factor in tumour growth. Nat Rev Cancer 2: 38-47.

28. Semenza GL (2003) Targeting HIF-1 for cancer therapy. Nat Rev Cancer 3: 721-732.

29. Cao S, Yang S, Wu C, Wang Y, Jiang J, et al. (2014) Protein expression of hypoxia-inducible factor-1 alpha and hepatocellular carcinoma: a systematic review with meta-analysis. Clin Res Hepatol Gastroenterol 38: 598-603.

30. Chen R, Xu M, Nagati JS, Hogg RT, Das A, et al. (2015) The acetate/ACSS2 switch regulates HIF-2 stress signaling in the tumor cell microenvironment. PLoS One 10: e116515.

31. Majmundar AJ, Wong WJ, Simon MC (2010) Hypoxia-inducible factors and the response to hypoxic stress. Mol Cell 40: 294-309.

32. Lim JH, Chun YS, Park JW (2008) Hypoxia-inducible factor-1alpha obstructs a Wnt signaling pathway by inhibiting the hARD1-mediated activation of beta-catenin. Cancer Res 68: 5177-5184.

33. Sahlgren C, Gustafsson MV, Jin S, Poellinger L, Lendahl U (2008) Notch signaling mediates hypoxia-induced tumor cell migration and invasion. Proc Natl Acad Sci U S A 105: 6392-6397.

34. Samulitis BK, Landowski TH, Dorr RT (2009) Inhibition of protein synthesis by imexon reduces HIF-1alpha expression in normoxic and hypoxic pancreatic cancer cells. Invest New Drugs 27: 89-98.

35. Yang J, Zhang X, Zhang Y, Zhu D, Zhang L, et al. (2016) HIF-2α promotes epithelial-mesenchymal transition through regulating Twist2 binding to the promoter of E-cadherin in pancreatic cancer. J Exp Clin Cancer Res 35: 26.

36. Zhang Q, Bai X, Chen W, Ma T, Hu Q, et al. (2013) Wnt/beta-catenin signaling enhances hypoxia-induced epithelial-mesenchymal transition in hepatocellular carcinoma via crosstalk with hif-1alpha signaling. Carcinogenesis 34: 962-973.

37. Fu OY, Hou MF, Yang SF, Huang SC, Lee WY (2009) Cobalt chloride-induced hypoxia modulates the invasive potential and matrix metalloproteinases of primary and metastatic breast cancer cells. Anticancer Res 29: 3131-3138.

38. Lopez-Sanchez LM, Jimenez C, Valverde A, Hernandez V, Penarando J, et al. (2014) CoCl2, a mimic of hypoxia, induces formation of polyploid giant cells with stem characteristics in colon cancer. PLoS One 9: e99143.

39. Zhang B, Guo W, Yu L, Wang F, Xu Y, et al. (2013) Cobalt chloride inhibits tumor formation in osteosarcoma cells through upregulation of HIF-1alpha. Oncol Lett 5: 911-916.

40. Maxwell PH, Wiesener MS, Chang GW, Clifford SC, Vaux EC, et al. (1999) The tumour suppressor protein VHL targets hypoxia-inducible factors for oxygen-dependent proteolysis. Nature 399: 271-275.

41. Wells A, Yates C, Shepard CR (2008) E-cadherin as an indicator of mesenchymal to epithelial reverting transitions during the metastatic seeding of disseminated carcinomas. Clin Exp Metastasis 25: 621-628.

42. Ashaie MA, Chowdhury EH (2016) Cadherins: The Superfamily Critically Involved in Breast Cancer. Curr Pharm Des 22: 616-638.

43. Bai L, Yu Z, Zhang J, Yuan S, Liao C, et al. (2016) OLA1 contributes to epithelial-mesenchymal transition in lung cancer by modulating the GSK3β/snail/E-cadherin signaling. Oncotarget 7: 10402-10413.

44. Elmansuri AZ, Tanino MA, Mahabir R, Wang L, Kimura T, et al. (2016) Novel signaling collaboration between TGF-α and adaptor protein Crk facilitates EMT in human lung cancer. Oncotarget.

45. Lombaerts M, van Wezel T, Philippo K, Dierssen JW, Zimmerman RM, et al. (2006) E-cadherin transcriptional downregulation by promoter methylation but not mutation is related to epithelial-to-mesenchymal transition in breast cancer cell lines. Br J Cancer 94: 661-671.

46. Natalwala A, Spychal R, Tselepis C (2008) Epithelial-mesenchymal transition mediated tumourigenesis in the gastrointestinal tract. World J Gastroenterol 14: 3792-3797.